Modeling the Mpemba Effect
Math 512- Milestone 5
12/6/04

Math Freezing Team

December 7, 2004

1 Introduction

This report looks at various phenomenon of ice freezing either quicker or slower depending on initial temperatures. It has been well documented under certain conditions that warm water will freeze quicker than cooler water when put in a freezer[6]. This behavior was first documented by Mpemba in 1969 by a young school student[6]. The purpose of this project is to verify this behavior, experiment with various factors that may affect this rate of cooling, and finally to try to mathematically model this behavior. If the factors of this behavior can be directly pinpointed and modeled, the Mpemba Effect would have a variety of useful applications[3]. One such application is demonstrated by our partner group in the Food Science Department looking for ways to freeze ice cream more efficiently.

This report will examine our progress over the semester, and put the progress into an overall prospective of what work remains to be done in the future. In Section 2, we review the literature in order to either present possible explanations to the Mpemba Effect, or to rule out possible solutions. We have also listed assumptions we have needed to make in order to mathematically model the process of ice freezing. In Section 3, we look at the development of our current model with a forced mixing term. This model shows that if the thermal mixing within a warmer fluid is large enough, it can freeze faster than a cooler liquid, thus showing the Mpemba Effect. In Section 4 we look at our continued efforts to make our data as reliable as possible and then take a look at several cooling curves as some base data. We also look at an experiment we performed to show that thermal mixing was happening in the fluid as it cooled. The report then draws conclusions between our mathematical model and our observed behavior. Finally, the report points out the current strengths and weaknesses of the project thus far and presents a proposal for future work.

2 Current Assumptions and Literature Review

The following is a list of model simplifications that were made as a result of the literature review. These eliminations were used primarily to rule out possible explanations of the Mpemba Effect, allowing us to focus our experimentation as much as possible.

- We have assumed that the presence of different amounts of dissolved oxygen does not have a large effect of the freezing process. We had read some literature by Jeng that suggested warmer water would hold less dissolved gas and resultantly freeze faster[5]. However, we have also come across a study by Deeson where this theory was tested and found that water with a normal concentration of dissolved gas froze the quickest [2].
- The difference of the amount of frost formation depending on internal temperature does not effect the thermal conductivity of the container.
  It was originally proposed by Douglas that the formation of frost would inhibit conduction from thermo-cooler to the container [4]. However, it is widely noted that frost does not have a major effect on thermal conduction.
- The greater amount of evaporation of the warmer water does not have a significant enough effect to justify the Mpemba Effect.
  We had read san article by Firth that suggested the decrease in mass due to evaporation could result in warmer water freezing quicker[5]. However, this theory has also been widely disproved. Our experimentation in the lab has also shown us that the change in mass has been negligible.

Several more assumptions listed in Section 3 had to be made for simplifications in the mathematical modeling section.

3 Mathematical Model and Assumptions

3.1 Base Case: Conduction Only

Our initial goal was to model the physics as simply as possible as a base case. Here we model the cooling of the water as if there were no Mpemba effect, using only conduction, starting from first principles.

3.1.1 Base Case Assumptions

The following is a list of assumptions we have made based on the physics of our experiment:

- There is no radiative heat transfer. This is not a blackbody and its temperature will never differ greatly from that of the surroundings.

- There is no kinetic energy flowing out of the system because all of the water stays inside during the entire experiment.
- There is no pressure work done on the system since its boundaries are in contact with the atmosphere, and the crucible is small enough to neglect hydrostatic pressure effects.
- There is no viscous work done within the system, since water is not a viscous fluid.
- There is no work done on the system by body forces, since the center of mass of the system remains stationary.
- There is no work done on the system by surface forces, since the surfaces of the system do not deform.
- $\hat{C}_P$, ρ, and k for water over the temperature range 263 K to 373 K can be averaged and taken as a constant since it does not vary much over the temperature range.

The following is a list of assumptions we have made so that we can successfully model conductive cooling:

- For the time being, assume only conductive cooling, because this is the main mode of heat transfer out of the system.
- Assume that the fluid has a uniform velocity of $\mathbf{0}$ throughout the system.

3.1.2 Development of Model for Base Case

The phenomenon we are exploring can best be described using heat transfer. A logical start to this investigation is to figure out how heat is lost in cooling. Since our experimental setup, at its simplest, is a warmer body in contact with a colder body, let us start with an expression for heat flux. The heat flux out of a body, $Q|_S$ is defined as follows:

$$Q|_S = \int_S (\mathbf{q} \cdot \mathbf{n})\, dA \tag{1}$$

where $\mathbf{n}$ is the unit outward normal vector on the control surface S, a convention that will be followed throughout the remainder of this paper. Also, as a matter of convention, the heat flux is positive when heat is flowing *out* of the system. Fourier's Law of Conduction gives an expression for the heat flux vector. It is stated as follows:

$$\mathbf{q} = -k\nabla T \tag{2}$$

where k is the thermal conductivity, and T is the temperature of the system. Since heat flux is an energy flow out of a system with control volume V bounded by a control surface S, one can apply an energy balance to the system:

$$\frac{\partial E}{\partial t}|_V + \dot{E}|_S = -Q_k|_S + \dot{W}|_{S,V} \tag{3}$$

The terms in the equation above are defined as follows:

- $\frac{\partial E}{\partial t}|_V$ signifies the change in the internal energy of the control volume over time.
- $\dot{E}|_S$ represents the net rate of energy flow *out* of the control surface due to convection.
- $-Q_k|_S$ refers to the negative of the conductive heat flow *out* through the control surface.
- $\dot{W}|S, V$ represents the combined rate of surface and volumetric work done *on* the control surface.

Rearranging and subdividing terms yields:

$$Q|_S = -\frac{\partial E}{\partial t}|_V - \dot{E}_u|_S + \dot{W}_p|_S + \dot{W}_\mu|_S + \dot{W}_{g,e}|_V + \dot{S}_e|_V \tag{4}$$

The seven terms, from left to right, break down as follows:

- $Q|_S$ denotes the total heat flux *out* of the control surface.
- $-\frac{\partial E}{\partial t}|_V$ is the change in internal energy within the control volume with respect to time.
- $\dot{E}_u|_S$ represents the negative of the net rate of kinetic energy flowing *out* of the control surface.
- $\dot{W}_p|_S$ signifies the rate of pressure work done *on* the control surface.
- $\dot{W}_\mu|_S$ represents the rate of viscous work done *on* the control surface.
- $\dot{W}_{g,e}|_V$ denotes the rate of gravitational and electromagnetic work done *on* the control volume.
- $\dot{S}_e|_V$ refers to the rate of any other type of work or conversion of energy done *on* the control volume.

Substituting the constituents into (4), these terms, in the same order, are further expressed as follows:

$$\begin{aligned} \int\limits_S (\mathbf{q} \cdot \mathbf{n})\, dA = -\frac{\partial}{\partial t} \int\limits_V (\rho e + \frac{\rho}{2}\mathbf{u} \cdot \mathbf{u})\, dV - \int\limits_S \frac{\rho}{2}(\mathbf{u} \cdot \mathbf{u})(\mathbf{u} \cdot \mathbf{n})\, dA - \int\limits_S (P\mathbf{u} \cdot \mathbf{n})\, dA \\ + \int\limits_S (\mathbf{S}_\mu \cdot \mathbf{u}) \cdot \mathbf{n}\, dA + \int\limits_V (\rho\mathbf{g} \cdot \mathbf{u} + \mathbf{f}_e \cdot \mathbf{u})\, d + \int\limits_V \dot{s}_e\, dV \end{aligned} \tag{5}$$

This equation is presented to show the rigorous physics involved in the situation before making simplifications to the model. In this base case, the goal is to obtain the heat equation. By showing the physical motivation behind the heat equation, we can then return to equation (5) to add additional terms without having to start a completely new derivation. The heat equation is provided as the base case model because it is a canonical PDE. It will be used to as a baseline model, since numerical results from later models will not vary significantly from the numerical results obtained from the heat equation.
According to the assumptions for the base case model:

- The last half of the second term is zero due to the assumption that $\mathbf{u} = \mathbf{0}$
- The third term is zero because no fluid leaves the system.
- The fourth term is zero because there is no pressure work done on the system.
- The fifth term is zero because water is a Newtonian fluid, and thus does not have significant viscous forces.
- The sixth term is zero because the center of mass of the system is stationary, so no gravitational or electromagnetic work could have been done on the system.
- The seventh term is neglected because no "other" work has been done on the system.

After cancellations, the energy balance reduces to:

$$\int_S (\mathbf{q} \cdot \mathbf{n}) \, dA = -\frac{\partial}{\partial t} \int_V \rho e \, dV \tag{6}$$

Applying the Divergence Theorem, Fourier's Law of Conduction, and canceling signs yields:

$$\int_V (\nabla \cdot k\nabla T) \, dV = \frac{\partial}{\partial t} \int_V \rho e \, dV \tag{7}$$

Rearrange to combine the arguments of the integrals over the control volume, passing the time derivative inside the volume integral:

$$\int_V ((\nabla \cdot k\nabla T) - \frac{\partial(\rho e)}{\partial t}) \, dV = 0 \tag{8}$$

Since this holds for any arbitrary control volume, the argument of the volume integral must be zero at every point within the control volume, thus:

$$\nabla \cdot k\nabla T - \frac{\partial(\rho e)}{\partial t} = 0 \tag{9}$$

From thermodynamics, the specific internal energy of the system can be defined as:

$$e(T) = \int_0^T \hat{C_V}(s) \, ds \tag{10}$$

where $\hat{C_V}$ is the specific heat capacity of the material under study at constant volume, and by convention, the specific internal energy content of a material at absolute zero. Since the material of interest is water, which is a liquid or solid during the experiment, this can be approximated by the specific heat capacity of water at constant pressure, $\hat{C_P}$, which is more easily measured. Since we have assumed that $\hat{C_P}$ is the average heat capacity of water between 263 K and 373 K, $e(T) = \hat{C_P}T$. This allows the energy balance to be simplified to the model for water cooled by conduction only:

$$\frac{\partial T}{\partial t} = \alpha \nabla^2 T \tag{11}$$

3.1.3 Solution of the Model for the Base Case

Solution of (11) proceeded by nondimensionalizing the variables in the system as follows:

- Define nondimensional radial coordinate, $\bar{r} = \frac{r}{R}$
- Define nondimensional vertical coordinate, $\bar{z} = \frac{z}{R}$
- Define nondimensional time, $\bar{t} = \frac{\alpha t}{R^2}$
- Define nondimensional temperature, $\bar{T} = \frac{T}{T_f}$

In cylindrical coordinates, nondimensionalizing (11) yields

$$\frac{\partial \bar{T}}{\partial \bar{t}} = \nabla^2 \bar{T} \tag{12}$$

The following boundary conditions arose from physical constraints:

- Continuity implies that $\frac{\partial \bar{T}}{\partial \theta}(\bar{r}, 0, \bar{z}, \bar{t}) = \frac{\partial \bar{T}}{\partial \theta}(\bar{r}, 2\pi, \bar{z}, \bar{t})$ and $\mathrm{\bar{T}}(\mathrm{\bar{r}}, 0, \mathrm{\bar{z}}, \mathrm{\bar{t}}) = \mathrm{\bar{T}}(\mathrm{\bar{r}}, 2\pi, \mathrm{\bar{z}}, \mathrm{\bar{t}})$.
- $\mathrm{\bar{T}}(0, \theta, \mathrm{\bar{z}}, \mathrm{\bar{t}})$ must be bounded.
- $\frac{\partial \bar{T}}{\partial \bar{z}}(\bar{r}, \theta, \frac{h}{R}, \bar{t}) = 0$, since there is no heat flux through the top of the container.
- $\frac{\partial \bar{T}}{\partial \bar{r}}(1, \theta, \bar{z}, \bar{t}) = 0$, since there is no heat flux through the sides of the container.
- $\mathrm{\bar{T}}(\mathrm{\bar{r}}, \theta, \mathrm{\bar{z}}, 0) = \mathrm{T_0/T_f}$ as an initial condition, where T_0 is the initial temperature of the water.
- Data taken from cooling curves suggests that there is a constant heat flux through the bottom of the container. This translates into $\frac{\partial \bar{T}}{\partial \bar{z}}(\bar{r}, \theta, 0, \bar{t}) = \frac{q_{flux} R}{k T_f}$.

Since the boundary conditions do not vary with theta except for continuity, assume an axisymmetric solution. Furthermore, since the boundary conditions have no radial dependence, assume that $\bar{T}$ is only a function of vertical position and time.

$$\bar{T}_{\bar{z}\bar{z}} = \bar{T}_{\bar{t}} \tag{13}$$

$$\bar{T}_{\bar{z}}(0, \bar{t}) = \frac{q_{flux} R}{k T_f} \tag{14}$$

$$\bar{T}_{\bar{z}}(\frac{h}{R}, \bar{t}) = 0 \tag{15}$$

$$\bar{T}(\bar{z}, 0) = \frac{T_0}{T_f} \tag{16}$$

The nonhomogeneous Neumann condition, $\frac{\partial \bar{T}}{\partial \bar{z}}(0,\bar{t})\frac{q_{flux}R}{kT_f}$, makes the use of separation of variables cumbersome with the equation as written. To fit the nonhomogeneous boundary condition, transform variables as follows:

$$\bar{T}(\bar{z},\bar{t}) = \frac{-q_{flux}R}{kT_f}\frac{(\bar{z}-\frac{h}{R})^2}{2\frac{h}{R}} + u(\bar{r},\bar{z},\bar{t}) \tag{17}$$

Carrying out the substitution, the problem becomes:

$$u_{\bar{z}\bar{z}} = u_{\bar{t}} + \frac{q_{flux}R}{kT_f} \tag{18}$$

$$u_{\bar{z}}(0,\bar{t}) = 0 \tag{19}$$

$$u_{\bar{z}}(\frac{h}{R},\bar{t}) = 0 \tag{20}$$

$$u(\bar{z},0) = \frac{T_0}{T_f} + \frac{q_{flux}R}{kT_f}\frac{1}{\frac{h}{R}} \tag{21}$$

At this point, it is easier to proceed by a further substitution,

$$u(\bar{r},\bar{z},\bar{t}) = u_1(\bar{r},\bar{z},\bar{t}) + u_2(\bar{r},\bar{z},\bar{t}) \tag{22}$$

This further eases the solution of the PDE, as seen below. Start with the u_2 problem, for simplicity:

$$u_{2\bar{z}\bar{z}} = u_{2t} + \frac{q_{flux}R}{kT_f}\frac{1}{\frac{h}{R}} \tag{23}$$

$$u_{2\bar{z}}(0,\bar{t}) = 0 \tag{24}$$

$$u_{2\bar{z}}(\frac{h}{R},\bar{t}) = 0 \tag{25}$$

$$u_2(\bar{z},0) = 0 \tag{26}$$

By inspection, the solution to the u_2 problem is only a function of $\bar{t}$, thus:

$$u_2(\bar{t}) = \frac{-q_{flux}R}{kT_f}\frac{\bar{t}}{\frac{h}{R}} \tag{27}$$

Now, state the u_1 problem:

$$u_{1\bar{z}\bar{z}} = u_{1\bar{t}} \tag{28}$$

$$u_{1\bar{z}}(0,\bar{t}) = 0 \tag{29}$$

$$u_{1\bar{z}}(\frac{h}{R},\bar{t}) = 0 \tag{30}$$

$$u_1(\bar{z},0) = \frac{T_0}{T_f} + \frac{q_{flux}R}{kT_f}\frac{(\bar{z}-\frac{h}{R})^2}{2\frac{h}{R}} \tag{31}$$

Applying separation of variables, assume a solution of the form $u_1(\bar{z},\bar{t}) = Z(\bar{z})\Theta(\bar{t})$:

$$\frac{Z''}{Z} = \frac{T'}{T} \tag{32}$$

Assume periodic solutions, since one does not expect great (i.e. "exponential") variations in temperature within a container with insulation on all sides but one. Let the eigenvalues be κ, where κ is nonnegative. Then,

$$\frac{Z''}{Z} = -\kappa^2 \tag{33}$$

$$Z'' + \kappa^2 Z = 0 \tag{34}$$

$$Z(\bar{z}) = \begin{cases} A + B\bar{z}, \ \kappa = 0 \\ C\cos(\kappa\bar{z}) + D\sin(\kappa\bar{z}), \ \kappa \neq 0 \end{cases} \tag{35}$$

$$Z'(0) = 0 \Rightarrow B = 0 \text{ and } D = 0 \tag{36}$$

$$Z'\left(\frac{h}{R}\right) = 0 \Rightarrow \kappa = \frac{Rn\pi}{h}, \ n \,\epsilon\, \mathbb{Z}^+ \tag{37}$$

$$\frac{T'}{T} = -\kappa^2 \tag{38}$$

$$T' = -\kappa^2 T \tag{39}$$

$$T(\bar{t}) = F\exp(-\kappa^2\bar{t}) \tag{40}$$

$$u_1(\bar{z},\bar{t}) = M + L\cos(\kappa\bar{z})\exp(-\kappa^2\bar{t}) \tag{41}$$

Using separation of variables and Sturm-Liouville theory, a solution can be obtained for u_1:

$$u_1(\bar{z},\bar{t}) = \frac{T_0}{T_f} + \frac{q_{flux}h}{6kT_f} + \sum_{n=1}^{\infty} \frac{2hq_{flux}}{(n\pi)^2} \cos\frac{Rn\pi\bar{z}}{h} \exp\left(-\left(\frac{Rn\pi}{h}\right)^2 \bar{t}\right) \tag{42}$$

Substituting Equations 42 and 27 back into Equation 17 yields the final nondimensional solution for $\bar{T}$:

$$\bar{T}(\bar{z},\bar{t}) = \frac{T_0}{T_f} + \frac{q_{flux}h}{6kT_f} - \frac{q_{flux}R}{kT_f}\frac{(\bar{z}-\frac{h}{R})^2}{2\frac{h}{R}} - \frac{q_{flux}R}{kT_f}\frac{\bar{t}}{\frac{h}{R}} + \sum_{n=1}^{\infty} \frac{2hq_{flux}}{(n\pi)^2} \cos\frac{Rn\pi\bar{z}}{h} \exp\left(-\left(\frac{Rn\pi}{h}\right)^2 \bar{t}\right) \tag{43}$$

3.2 Second Case: Convection by Time-Invariant Mixing

The goal of this second model was to determine whether or not time-invariant mixing significantly affects the temperature distribution within the system. Here we model cooling by relaxing the assumption of a completely stagnant fluid by replacing it with an equation that describes the velocity of the fluid over the entire system. In doing this, we introduce convective heat transfer into the system.

3.2.1 New Terms for the Second Case

- Φ is the velocity potential of the fluid within the system and has units of [m^2/s]
- $\nabla\Phi = \mathbf{u}$

3.2.2 Assumptions for Second Case

The assumptions for the second case based on physical phenomena are the same as the list presented for the first case. The following is a list of assumptions we have made so that we can successfully model convective cooling:

- Assume the velocity potential of the fluid within the system is governed by the equation

$$\nabla^2\Phi = f(r, \theta, z) \tag{44}$$

- As a result of there being a nonzero fluid velocity in the system, assume there is conductive heat transfer within the system.

3.2.3 Development of Model for Second Case

Returning to the expanded energy balance in (4), we again cancel terms.

- V, an arbitrary control volume, moves with time.
- This time, $\mathbf{u} \neq \mathbf{0}$, so the last half of the second term does *not* drop out. Likewise, because the control volume moves, fluid does flow in and out of the system, so the third term must be included.
- The last four terms cancel as before.

Simplifying after cancellations:

$$\int\limits_S (\mathbf{q} \cdot \mathbf{n})\, dA = -\frac{\partial}{\partial t} \int\limits_V (\rho e + \frac{\rho}{2}\mathbf{u} \cdot \mathbf{u})\, dV - \int\limits_S \frac{\rho}{2}(\mathbf{u} \cdot \mathbf{u})(\mathbf{u} \cdot \mathbf{n}) \tag{45}$$

Applying the Divergence Theorem and substituting in the relations for conductive heat transfer, convective heat transfer, and the velocity yields:

$$\int\limits_V (\nabla \cdot k\nabla T)\, dV = \frac{\partial}{\partial t} \int\limits_V (\rho e + \frac{\rho}{2}\mathbf{u} \cdot \mathbf{u})\, dV - \int\limits_S \frac{\rho}{2}(\mathbf{u} \cdot \mathbf{u})(\mathbf{u} \cdot \mathbf{n}) \tag{46}$$

One then has to apply the Reynolds Transport Theorem, a generalization of the Leibniz Rule to three dimensions:

$$\int\limits_{V(t)} (\nabla \cdot k\nabla T)\, dV = \int\limits_{V(t)} \frac{\partial(\rho e + \frac{\rho}{2}\mathbf{u} \cdot \mathbf{u})}{\partial t}\, dV + \int\limits_{S(t)} (\rho e + \frac{\rho}{2}\mathbf{u} \cdot \mathbf{u})(\mathbf{u} \cdot \mathbf{n})\, dA - \int\limits_{S(t)} \frac{\rho}{2}(\mathbf{u} \cdot \mathbf{u})(\mathbf{u} \cdot \mathbf{n}) \tag{47}$$

Since $\mathbf{u}$ does not vary with time and ρ is constant, we can cancel terms:

$$\int\limits_{V(t)} (\nabla \cdot k\nabla T)\, dV = \int\limits_{V(t)} \rho \frac{\partial e}{\partial t}\, dV + \int\limits_{S(t)} (\rho e)(\mathbf{u} \cdot \mathbf{n})\, dA \tag{48}$$

Again, we apply the Divergence Theorem to the surface integral term:

$$\int\limits_{V(t)} (\nabla \cdot k\nabla T)\, dV = \int\limits_{V(t)} \rho \frac{\partial e}{\partial t}\, dV + \int\limits_{V(t)} \nabla \cdot (\rho e\mathbf{u})\, dV \tag{49}$$

Now, use the product rule to expand the right-hand side:

$$\int\limits_{V(t)} (\nabla \cdot k\nabla T)\, dV = \int\limits_{V(t)} \rho \frac{\partial e}{\partial t}\, dV + \rho \int\limits_{V(t)} (\nabla e \cdot \mathbf{u} + e\nabla \cdot \mathbf{u})\, dV \tag{50}$$

Since, by definition, $\mathrm{div}(\mathbf{u}) = 0$:

$$\int\limits_{V(t)} (\nabla \cdot k\nabla T)\, dV = \int\limits_{V(t)} \rho \frac{\partial e}{\partial t}\, dV + \rho \int\limits_{V(t)} \nabla e \cdot \mathbf{u}\, dV \tag{51}$$

Since this holds for any arbitrary control volume, V, arguments of the integrals on both sides must be equal, thus:

$$\nabla \cdot k\nabla T = \rho(\frac{\partial e}{\partial t} + \nabla e \cdot \mathbf{u}) \tag{52}$$

3.3 Future Modeling Goals

We believe that if the internal velocity of the fluid is large enough in a warm fluid, it can cool quicker than a fluid with a lower initial temperature. To show this, we can apply the model above, replacing the general function, f, in Equation 44 with an appropriate forcing function that gives the "curling" effect expected in convection. Equations 44 and 52 could then be solved analytically, yielding a solution for temperature that more closely approximates our experimental data. The last step of modeling the Mpemba Effect is to find a correlation between the internal fluid velocity and its initial temperature. We propose using the Boussinesq approximation, which has been used to describe all nonisothermal, free convective flows.[1] This must be solved using either using a numerical PDE solver or a software simulation package. Once we can tie together a fluid's temperature to its internal mixing velocity, we can determine if higher temperatures induce greater mixing velocities, which in turn excite convective modes of heat transfer, as we hypothesize. This will then show that convection causes the Mpemba Effect, and we should be able to accurately predict lab results.

4 Experimentation Results

So far we have completed four separate experiments in the MEC lab. All four experiments used the same basic "tower" setup, however the first experiment was performed without the experiment stand, clamp and glass tubes. The "tower" setup begins with a base platform with a cooling fan. Stacked on top of the cooling fan is the heat sink followed by the thermoelectric cooler, conductive paste, and finally crucible. The thermoelectric cooler and cooling fan are both powered by DC power supplies. In the final three experiment, a lab stand is butted up against the base platform. Attached to the lab stand is a clamp that holds two hollow, glass tubes. Through these tubes, the wires from the thermo-couples are fed. Tape with markings is also added for the third experiment in order to attempt to measure the heat flux in the water. The lab setup used is shown in Figure 1.

At the recommendation of thermodynamics professor, Dr. Mulders, our first experimental goal was to establish a basis that would make our future results more solid. For our basis, we recorded the cooling curves for 5 mL of room temperature (20 degrees Celsius) water. Our first effort at the basis was not very successful. As a group, we came to the conclusion that the lack of consistency was due to the thermocouple not being positioned in the same location in the crucible each time. We fixed this issue in our second attempt at the basis by adding the lab stand and clamp. Our results from the second trial were much more reliable. A comparison of the initial results to our current results are shown in Figures 2-3.

The second experiment that we performed used two thermo-couples simultaneously. One thermocouple was placed in the crucible and the other placed on the surface of the thermoelectric cooler. The purpose of this experiment was to test the heat flux of our system by changing the height of the thermocouple within the crucible at constant increments and measuring the temperature difference between the two thermo-couples. The difference between the thermo-couples appeared to be relatively constant throughout the cooling process. One of the trials from this experiment is shown in Figure 4. This graph shows a relatively constant difference in temperature between the two thermocouples of three degrees Celsius. Because we know the distance between the two thermocouples and the heat transfer coefficient of water, we can can calculate the heat flux in the system.

$$q_{flux} = .59 * \frac{3}{.006} = 295W \tag{53}$$

This calculation was used in conjunction with out conduction model to see how accurate a solution we could get ignoring convection. Once we had calculated our heat flux into the system, we could compare our theoretical results to out actual lab data. However, we saw that our model based only on conduction did not give an accurate portrayal of the freezing behavior in the water. Although our theoretical model has the same general trends as our experimental model, we can clearly see that the two theoretical cooling curves will not intersect. This shows that our theoretical model is missing key elements that would allow it to better portray the Mpemba Effect.

The third experiment we did in the MEC lab was to freeze water at different initial temperatures. We hoped to see that the warmer water would freeze faster than the cooler water, thus illustrating the Mpemba Effect. We did three different tests, freezing 1 mL water at several different initial temperatures. We saw that the warm water did indeed freeze quicker than the water with a cooler initial temperature. These results are shown in Figure 6. Although we were happy to see the Mpemba Effect, we found these results to be unreliable. We repeated the experiment three weeks later and were unable to repeat this behavior. This may have been due to inconsistencies in our lab setup, or some outside interaction we failed to identify.

The final experiment we did was to determine if there was an internal fluid velocity in the water as it cooled. We believe that the Mpemba Effect occurs because of different amounts of convective heat transfer between liquids with different initial temperatures. However, in order for this convection to take place, there must be some amount of mixing velocity within the fluid. If there was no mixing within the fluid, the temperature at each depth should be constant. Because the outer boundaries of the crucible were insulated, the heat flux must be constant at each depth. This type of temperature distribution is shown in Figure 7.

We designed an experiment to measure the temperature of the fluid in two horizontal locations at the same depth. We set up a thermocouple in the center of the crucible, and another 2 mm offset from the center. We repeated this experiment at depths of 2, 4, and 6 mm from the bottom of the crucible. While the initial temperatures at each of these locations started equal, the temperature difference between the two reached a maximum value after about 30 seconds and remained constant as the water cooled. A sample of this behavior is shown in Figure 8. Our experimental results are shown in figure 9. We found that the temperature was not constant at each particular depth, and thus there is some internal mixing going on as the fluid cools. We believe the temperature distribution in the fluid looks more like Figure 10 than Figure 7. This shows that convection does occur in the liquid and may be the cause of the Mpemba Effect.

5 Current Strengths and Weaknesses

Our current project was separated in two major areas; the mathematical modeling portion and the experimental modeling portion. Each of these two areas have separate strengths and weaknesses. These weaknesses should be worked on in the future to continue to move the project forward.

Within the modeling, our biggest strength is that we have successful modeled the heat equation in a cylinder with appropriate boundary conditions and included a mixing term. We have also believe that a fluid with a large enough internal mixing term can cool quicker than a fluid with a lower initial temperature, but less mixing. The major weakness is that this model accounts for a induced mixing, but not necessarily a internal velocity that directly ties to the fluids temperature. In the future, we would like to show that the initial temperature of the fluid determines the internal velocity, and determine this relationship.

In the experimentation section, our biggest strength is that we have seen the Mpemba Effect, and have also shown that their are mixing currents within the fluid as it cools. Our biggest weakness is that we have not be able to experimentally determine the magnitude of this velocity or connect it to a specific initial temperature. We have also not be able to build a setup that always demonstrates the Mpemba Effect.

6 Future Work

This report has successfully shown that that Mpemba Effect can be created, and that convection is an important mode of heat transfer in the fluid. We have also developed a model to show that with enough internal mixing, the convective heat transfer can make a warmer liquid cool fasted than a cooler one. The last step in completing this project is to show the relationship between the fluid's temperature and its internal velocity and solve our model as a coupled PDE. We will then be able to see wether convection though thermal mixing explains the Mpemba Effect. Below is a list of suggestions for future work with this project.

- Determine a correlation between the internal velocity of the fluid and the temperature in order to complete the mathematical model.
- Determine the amount of convective heat transfer that can take place for a fluid at any given initial temperature, and find the optimal initial temperature for the quickest freezing time.
- Compare our mathematical data to our actual lab data to see if the model can accurately predict the Mpemba Effect.

References

[1]

[2] Eric Deeson. Cooler- lower down. *Newman College of Education.*

[3] Dr. H. Douglas. Theoretical aspects of the freezing process.

[4] I.Firth. Cooler? *Physics Education*, 6(1):32–41, January 1971.

[5] Monwhea Jeng. Can hot water freeze faster than cold water? University of California Department of Physics, 1998.

[6] E.B. Mpemba and D.G. Osborne. Cool? *Physics Education*, 4(3):172–175, May 1969.

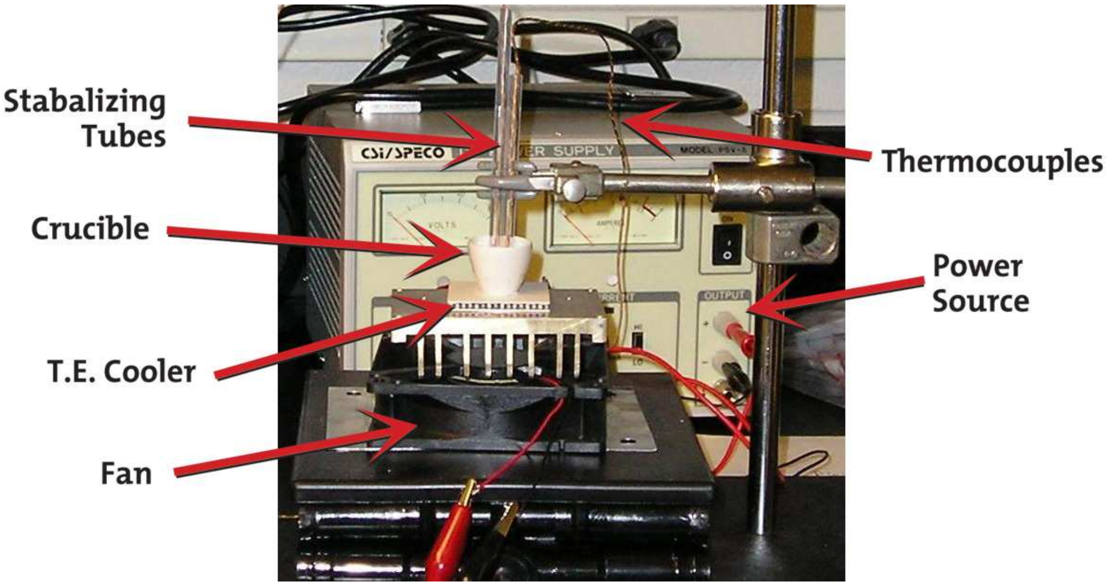

Figure 1: Above is the lab setup used in the MEC lab. The clamped glass tubes allow us to hold the thermo-couples in place more accurately.

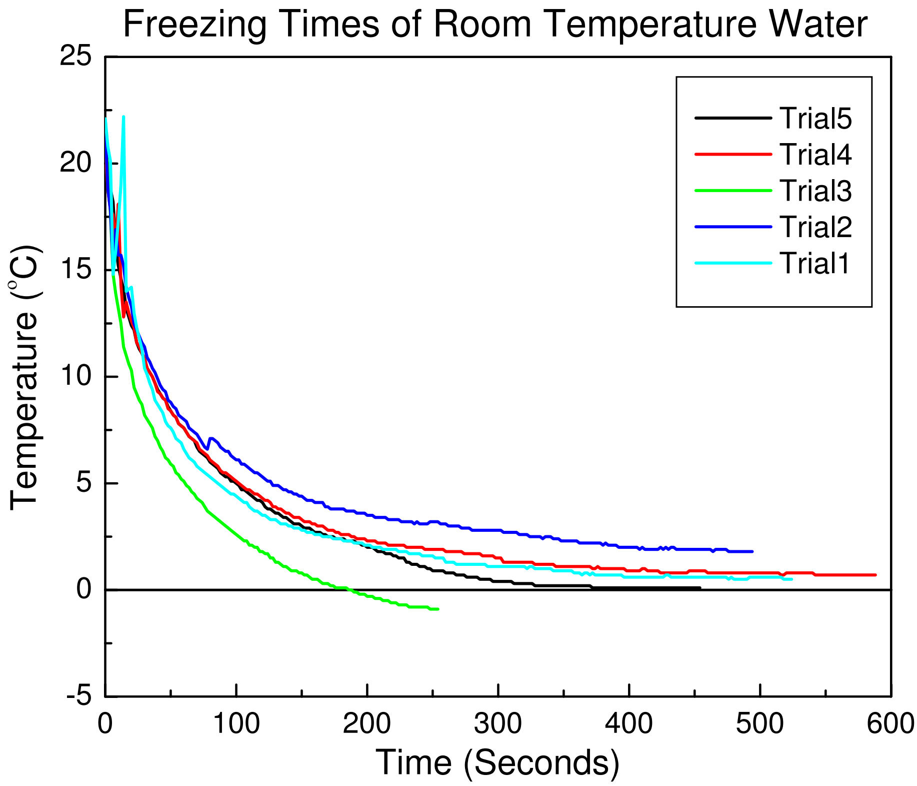

Figure 2: The graph above shows our cooling data we took before refining our setup. Notice that while all the initial conditions are the same, the variability in our setup caused us to get very inconsistent data.

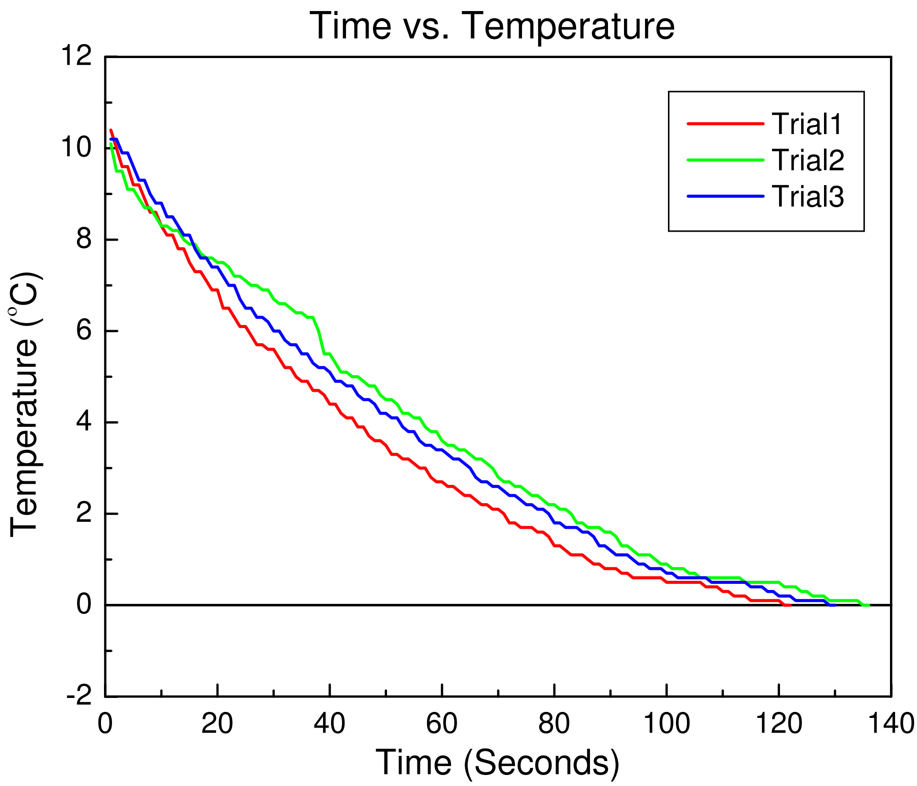

Figure 3: The graph above shows several cooling curves of water with the same initial conditions after we refined our setup. Notice how much more repeatable our results became compared to our earlier accuracy test.

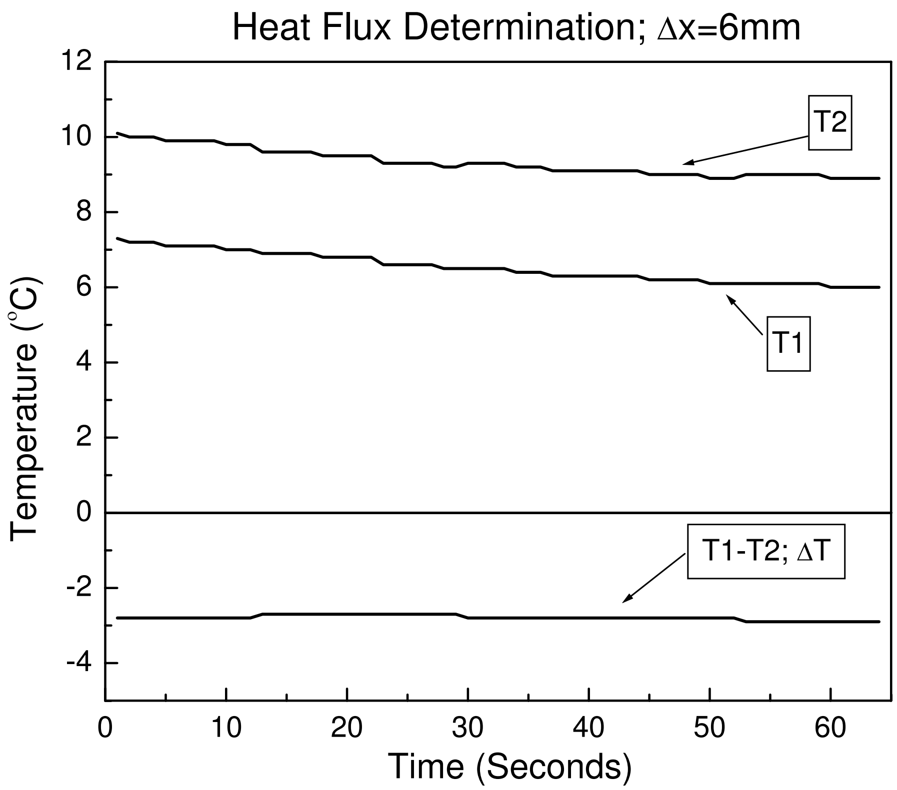

Figure 4: The graph above shows a sample we used to calculate the heat flux. Because we know dx, and we can see that dT is relatively constant throughout the cooling process, we can use the conduction equation to calculate the heat flux into the system.

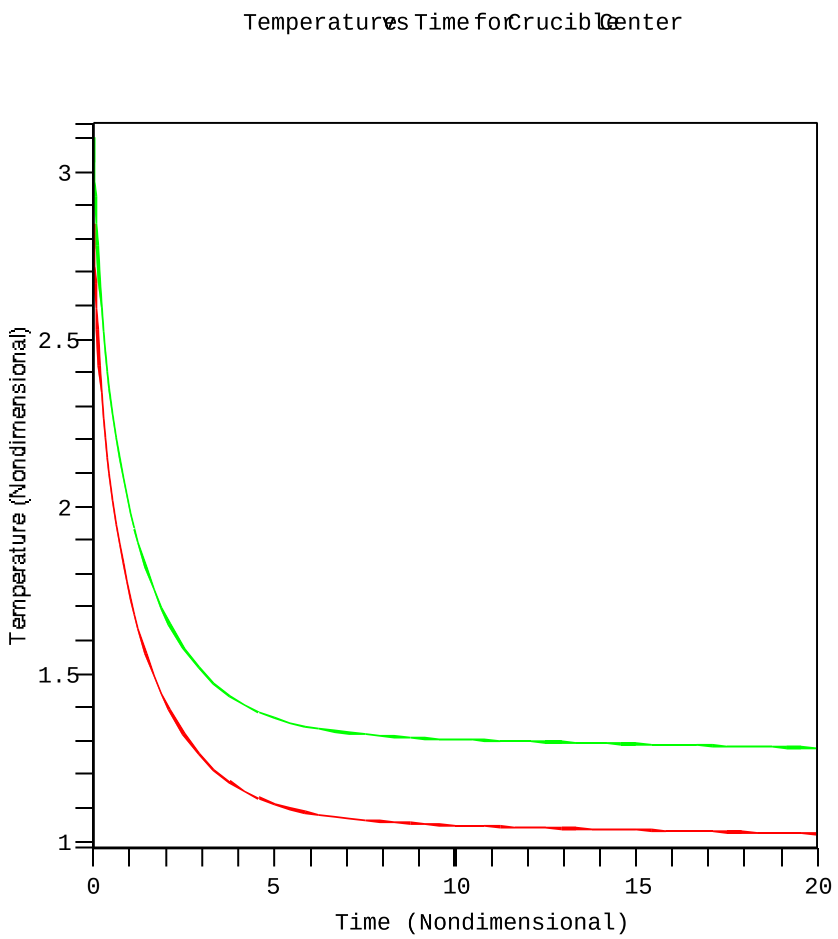

Figure 5: The graph above shows the theoretical results of our conduction only model for the water freezing at two different intimal conditions. While the general behavior of this model is the same as our lab data, the rate of cooling and freezing point are very different. This suggests convection plays an important role in the freezing process. Also notice that the two curves with different starting temperatures will not intersect, therefore, never demonstrating the Mpemba Effect.

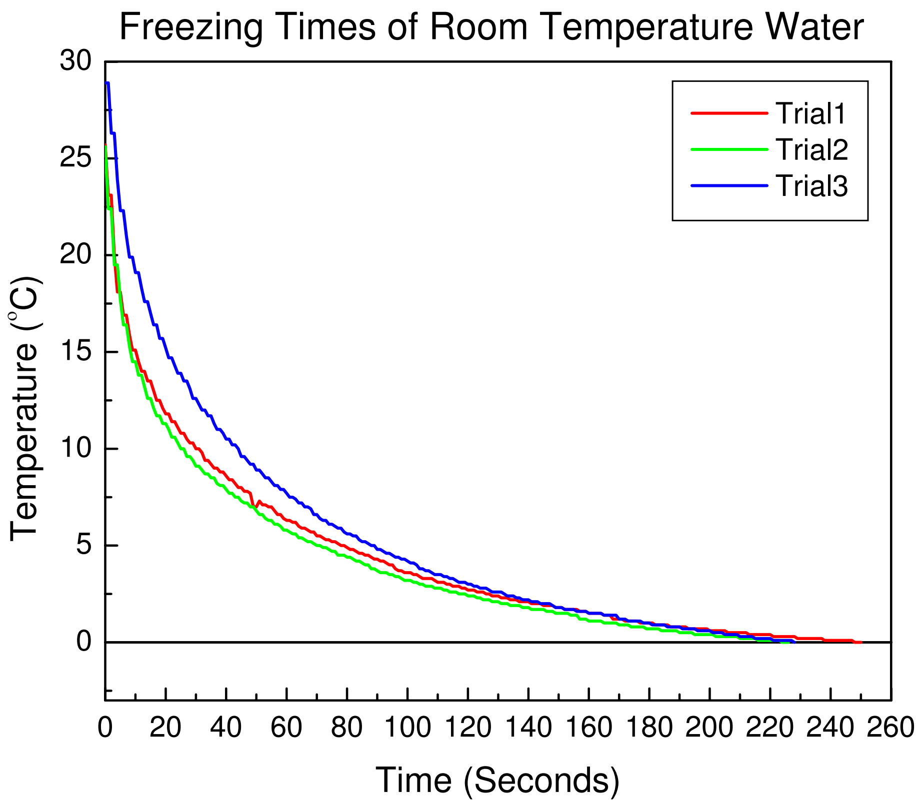

Figure 6: The graph above illustrates the Mpemba Effect. Notice that the water with the higher intimal temperature actually reaches freezing before the cooler samples.

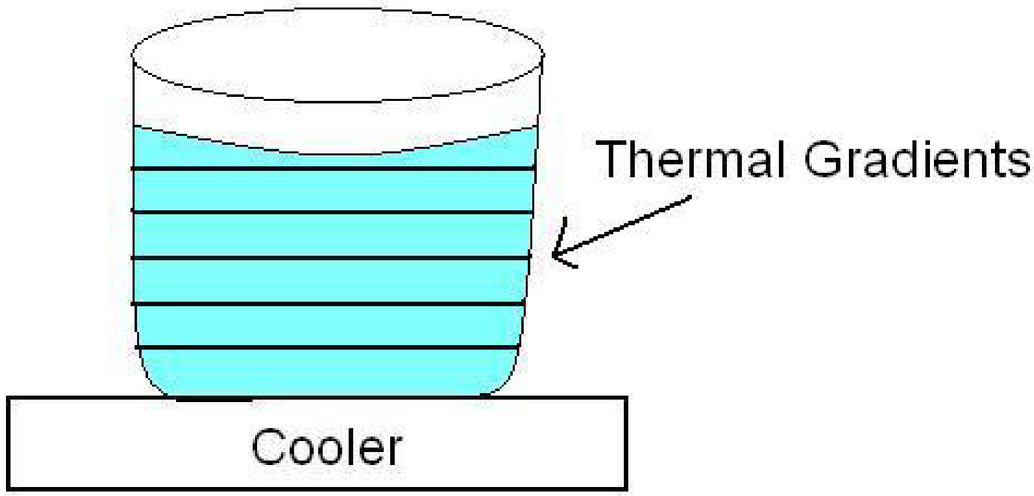

Figure 7: The graph above illustrates the thermal gradients that would occur if not convection or thermal mixing occurred within the fluid. Notice that the temperature is constant at each depth within the crucible.

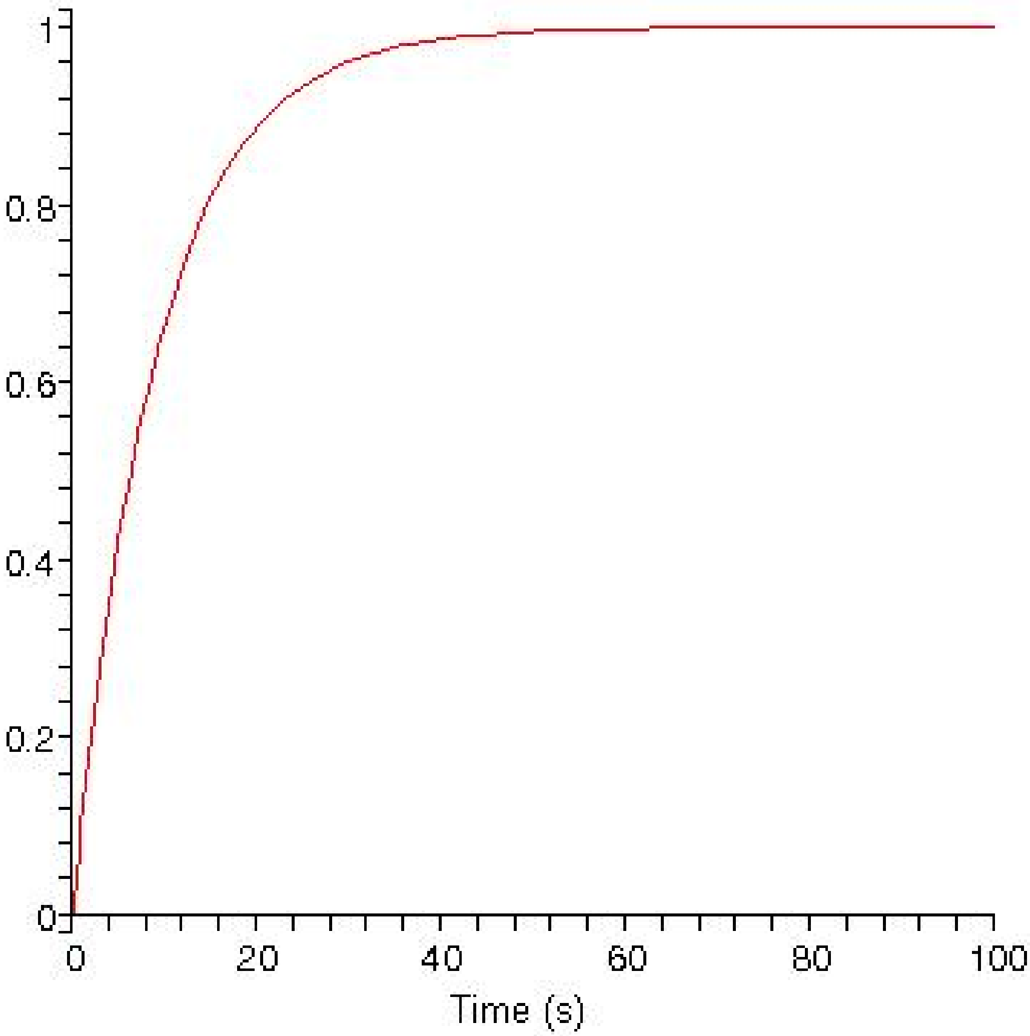

Figure 8: The graph above shows an example of the temperature difference at different locations within the crucible at the same depth. Notice that there is a difference in temperatures. This shows that some form of mixing must be present in the fluid.

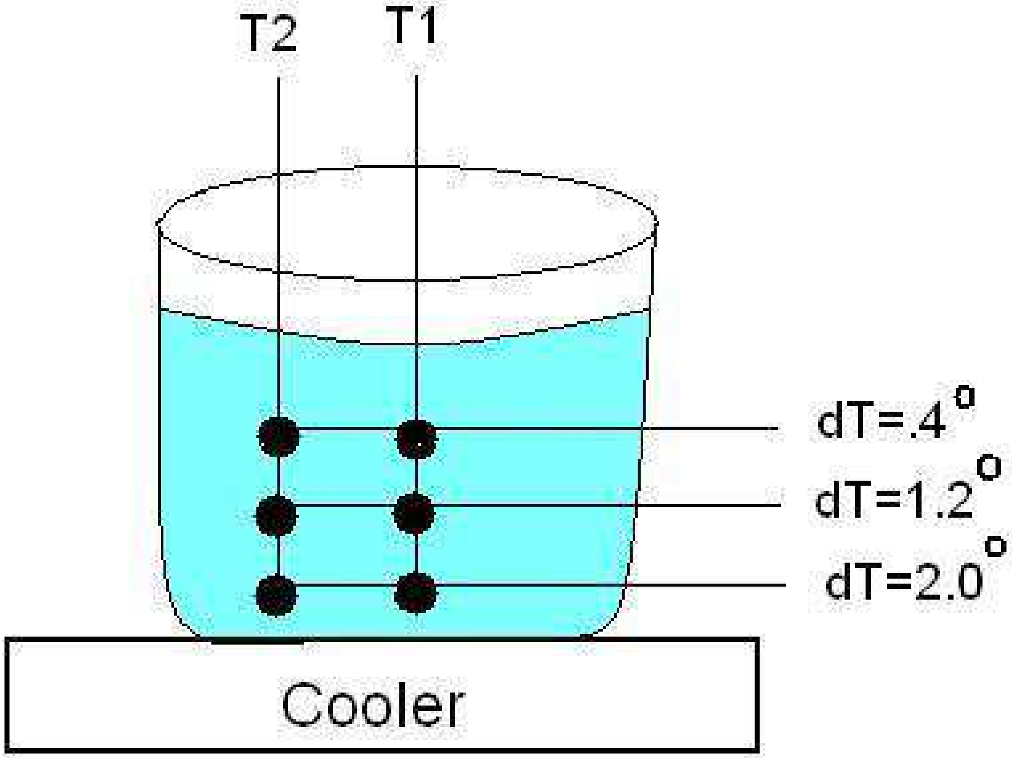

Figure 9: The picture above represents the results from our conduction experiment. Notice that the temperatures at each depth are not constant horizontally, indicating thermal mixing within the fluid.

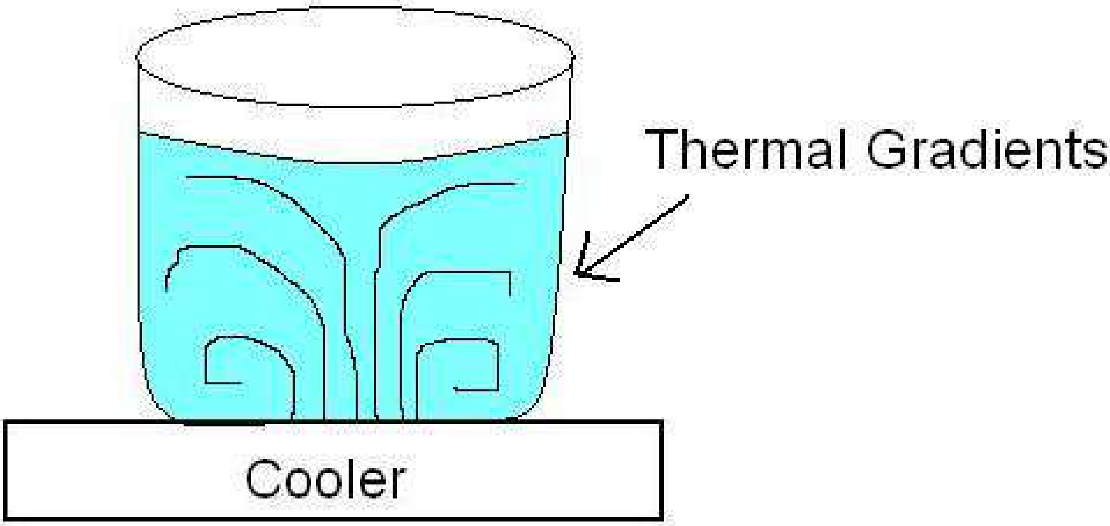

Figure 10: The picture above illustrates what we believe the thermal gradients within the fluid look like. Because they result in mixing within the fluid, it makes conductive heat transfer possible as the fluid cools.